

We are IntechOpen, the world's leading publisher of Open Access books Built by scientists, for scientists

4,800

Open access books available

122,000

International authors and editors

135M

Downloads

Our authors are among the

154

Countries delivered to

TOP 1%

most cited scientists

12.2%

Contributors from top 500 universities



WEB OF SCIENCE™

Selection of our books indexed in the Book Citation Index
in Web of Science™ Core Collection (BKCI)

Interested in publishing with us?
Contact book.department@intechopen.com

Numbers displayed above are based on latest data collected.
For more information visit www.intechopen.com



Planning and Sizing with OsiriX/Horos

Giovani José Dal Poggetto Molinari

Additional information is available at the end of the chapter

<http://dx.doi.org/10.5772/intechopen.78018>

Abstract

It is known that endovascular aneurysm repair (EVAR) requires a precise deployment of the graft and so the anatomical and morphological characteristic study of the aorta and its branches is mandatory. The increase of endovascular surgeons' interest on tomography image edition through software is marked specially when the increasing frequency of these procedures and its complexity have impelled surgeons to face additional and successive risk to occupational radiation exposure. Thus, a meticulous study of the angio-CT during EVAR preparation allows the reduction of unnecessary radiation exposure, as it also reduces consecutive image acquisition and contrast use (that may be related to renal overload in susceptible patients). Although some studies propose effective strategies to optimize the procedure, they rely on the use of additional specific and advanced equipment, available only in major centers. As an alternative, a simpler technique through image manipulation on the software OsiriX/Horos, aiming to reduce both exposures, is presented.

Keywords: EVAR, angio-CT, planning, sizing

1. Introduction

Over the last decades, since the first published results by Juan Parodi in 1991 [1], endovascular aneurysm repair (EVAR) became the vascular surgeon's most preferential technique to treat aortic aneurysms due to its benefit of early clinical and surgical outcomes with good long-term durability. EVAR has progressively replaced open surgical repair (OSR), especially in the infrarenal territory, representing currently over half of the surgeries for abdominal aneurysms [2, 3]. The development of new modern devices (with features that can adapt to different morphologic presentations of this aortic disease, which in the past were considered as not eligible for EVAR), like low-profile delivery systems, conformability and flexibility, has required some new aptitudes beyond endovascular skills for this type of repair, directly

related to specific technical knowledge of each brand's endograft and their usage facing each patient's anatomy.

Consequently, the image study in the pre-operative time took the uttermost importance in order to ensure the adequate selection of patient candidates for EVAR, the decision to endograft type and size, and additional details for postoperative follow-up. Different from OSR, EVAR relies on knowing the patient's anatomy well enough to choose the appropriate device preoperatively [4]. Adequate planning is an essential and indispensable step for technical success, in order to promote appropriate adjustment of the graft to the vessel wall and consequently aneurysm sac exclusion with blood flow reorientation [5, 6]. The implications of an inefficient planning can be seen immediately—or after the procedure—by endoleaks' formation or late aneurysm sac growth [6]. Even an underestimation of 2 millimeters in the vessel size can result in fixation and sealing failure, creating endoleaks, migration, and secondary interventions needs (including OSR conversion of late aortic rupture). Moreover, this step warrants the foreknowledge of additional surgical strategies for EVAR viability, like angioplasties, bypass or conduits, and hypogastric occlusion [4].

Therefore, it is important that the surgeon shows familiarity to all the necessary tools to perform a meticulous analysis of the computed tomography angiography (CTA), an imperative exam for this disease evaluation. Nowadays, the multislice CTA represents one of the most important methods for diagnostics and the assistance of vascular disorders. Its performance is related to modern attributions like better spatial and temporal resolution associated with the characteristic vascular lumen attenuation obtained by intravenous contrast injection [7]. CTA yields thinner tomographic segments that give high-definition properties to superior three-dimensional (3D) image reformatting, with the less use of iodinated contrast while captured under faster sweep for image generation [8]. A single intravenous bolus contrast injection can produce slices from thorax, abdomen, and pelvis, with a 0.5–1.5 millimeters thickness. When compared to the conventional angiography, the CTA is less expensive, less invasive, and exposes the patient to lesser radiation doses [9].

Also, technological refinements of these (thinner) slices provides plenty of details that—associated with software for image manipulation—promotes the study of large anatomical segments (including a complete patient's scan). These tomographic data, known as digital imaging and communications in medicine (DICOM) files, additionally retain information of radiation dose distribution at different levels (such as organs and other structures) that—associated with highly sensitive and precise algorithms of 3D-by-volume rendering—allows a patient's scan to be recreated in these software as interactive models along with their vascular anatomy [10, 11]. A range of data processing of the CTA-DICOM files can be practiced and are as follows: multiplanar reformats, bidimensional (2D) and 3D MPR and 3D MPR curved; minimal and maximal intensity projections, MinIP/MIP; 3D volume and surface rendering; and shaded surface display. Each one of these image formattings has its peculiarity and it is important to identify a specific arterial alteration in other distinct projections, rendered by different techniques [9]. There is no type of image reconstruction that is more effective than another; they all have their own properties and indications, where often it is necessary of more than just one kind to demonstrate properly a disease [7].

The preoperative analysis of the CTA consists of three principal purposes: to determine eligibility for EVAR, to choose the appropriate endograft, and to simulate a plan of intervention. Thereby, decisive information for EVAR execution is extracted—like the morphologic configuration of aneurysm's neck (tapered, reverse tapered, cylindrical, angulated, the presence of thrombus, etc.); the anatomy of visceral arteries related to the aortic axis (lowest renal artery—LRA); to set the anatomic areas for proximal and distal sealing and deployment of the graft and its diameters for device sizing; to access the quality of arterial paths (stenosis, tortuosities, vessel wall alterations, etc.); and to apprehend the possible necessity of auxiliary procedures for EVAR completion. These abilities raised the preparatory purpose of EVAR due to the many-times expressive and complex presentation of the arteries in the presence of aneurysmal disease [11, 12].

The most popular software used among vascular surgeons are OsiriX Imaging Software (Pixmeo Labs., Geneva, Switzerland) and the Aquarius iNtuition system (TeraRecon, Inc.) and both are retail versions [13]. Lately, the Horos software (horosproject.com) has been shown as a free downloadable option for OsiriX MD: It has the same interface and functionality, running on a 64-bit platform. Although Horos is a low-cost alternative for EVAR planning, only OsiriX and TeraRecon have FDA and CE Marking. The following techniques, described for image inspection for the EVAR study, can be reproduced in Horos, although to ensure its scientific validity OsiriX MD is recommended (FDA approved).

2. Understanding EVAR morphologic concepts

Necks are the proximal aortic and distal iliac segments free of aneurysmatic disease. It allows the grafts' adequate apposition and promotes the fabric's sealing to the vessel and stent fixation [6, 13]. By reason of the absence of suture to the artery, the durability and stability of EVAR depend almost exclusively on the stent's radial force and friction to the wall. This is why meticulous studies of aneurysms' necks are decisive.

a. The proximal neck:

The proximal neck of an infrarenal aneurysm is defined by the segment from immediately below the LRA to the beginning of the aortic dilation [14]. It can be analyzed by form, length, diameter, angulation, and related alterations (such as calcifications, ulcers, and thrombus) [13].

Form: Aneurysms' necks can exhibit forms as cylindrical, tapered, and reverse tapered. In cylindrical necks, the diameters' difference between the two extremities is inferior to 15%. Tapered necks display up to 20% of this variation, just as 20% is inversely proportional in reverse-tapered necks [14]. Necks over a 30% change in diameter and reverse tapered are not eligible for EVAR and a revision of treatment strategy should be considered into a more complex network that involves visceral arteries.

Length: The ideal neck's length, according to most of the grafts' instructions for use (IFU), is 15 mm. Some devices have active proximal fixation and can adapt to a 10 mm neck. Nevertheless, the shorter the neck the greater is the risk of type Ia endoleak. The ideal neck length is longer or equal to 20 mm [13, 15, 16].

Diameter: There are clear evidences that cranial progression of the aneurysmal disease can occur independently of the type of care (OSR or EVAR) [6]. Aortic necks over 30–32 mm are likely to be diseased and progress to proximal degeneration. They offer no durability to sealing and evolve in time to type Ia endoleaks and thus to reintervention needs [13, 16]. On the other hand, narrow necks (under 18 mm), although less frequent, must be carefully evaluated. Since the majority of endografts' size starts from 22 mm (which confers an above 20% of diameter oversize), there is potential exposure to wall stress, partial graft unfolding with fabric corrugation, and even aortic rupture [14]. Currently, the smallest available main body diameter device is the 20 mm Ovation Prime (Endologix Inc., Irvine, CA) [16]. The aortic bifurcation diameter should also be measured. Distal narrow aortic bifurcations (inferior to 20 mm) are not suitable to fit both iliac grafts and may compete for space leading to one of the leg thrombosis by compression exerted by the contralateral branch [17]. This can be avoided by aortic-monoiliac devices (with femoro-femoral bypass and contralateral proximal plug occlusion) or single-piece bifurcated grafts like AFX (Endologix Inc., Irvine, California) [14, 18].

Angulation: The suprarenal aneurysm's angle is defined as the suprarenal axis blood flow and aneurysm's neck. The infrarenal angle is determined between the aortic neck and the aneurysm axis [19]. It is important to specify these two curvatures once they have implications related to the bare-stent accommodation (i.e., the *free flow* in suprarenal fixations) and correct deployment of infrarenal stent graft. For the majority of commercially available devices, it is not recommended to exceed an angulation over 60 degrees, except for those specifically designed for 75–90 degrees angulated necks like Anaconda (Vascutek Terumo Lt., Scotland, UK) [20] and Aorfix (Lombard Medical Inc., Irvine, CA) [21]. There is a consistent risk of irregular deployment if these advices are not observed [13]. Patients with angled necks are more willing to present other associated morphologic alterations that may define technical challenge for EVAR execution. Severe angulations can result in endograft's kinking or migration along with a lower-than-the-ideal apposition site at the deployment time. Angled aortas should be pursued by the *functional neck*, that is, the length segment that can adequately suit the graft's sealing and fixation. Its limit is ruled by the internal curvature of these tortuous necks where the extra-stiff guide wire (e.g., Lunderquist) takes over its trajectory, especially when in short aortic necks. On the other side, in elongated necks, the curvature can be influenced by the stiffness of the wire, rectifying it. Under the influence of these wires, the longer the neck, the greater the probability of readjustment of the aortic axis and angle remodeling. For complex morphologic and severe angle presentations, oversizing the graft above 20% is mandatory [22]: when an endograft is implanted in an angulated aortic neck, it might not land perfectly in line with the vessel but rather angulated, which decreases the "effective" amount of oversizing. [23] Due to the probability of asymmetric deployment of the device (which tends to follow the guide wire path) the *functional neck* assumes a more elliptical shape—being necessary the election of larger main body diameters to guarantee uniformity of the stent-graft contact to the arterial wall [22].

Thrombus and calcifications: The presence of thrombus or atherosclerotic plaques over 50% or two-thirds of the neck's circumference prevents ideal proximal sealing, with potential type 1a endoleak evolution. Thus, EVAR is not recommended for these cases. Furthermore, it can cause atero/thrombo embolic complications by manipulating endovascular instruments (to visceral branches and distal arteries) [13, 14, 24]. On the presence of a heavily calcified neck, the Ovation Prime (Endologix Inc., Irvine, CA) becomes an alternative due to the polymer properties of filling the gaps between the vessel wall and the graft's fabric, warranting appropriate sealing [16].

b. The distal neck:

The distal neck is defined as the bottom site for endograft's anchorage and sealing. It can be analyzed by length, diameter, angulation with the aortic axis, and tortuosity of the access vessels (external iliac and femoral arteries).

Length: It should be longer than 10 mm. When given extreme tortuosity, longer lengths are recommended [6]. Thus, the greater the graft's area of contact to the arterial wall at the distal neck, the greater are the friction forces that will restrict stent migration and type 1b endoleaks [25]. Also, the most proximal to the hypogastric ostium is the prosthesis; the greater is the stability untowardly to its migration [26]. Along with the support, iliac fixation is associated with factors related to proximal migration of the endografts [27]. Short iliacs can lead to device unbalance and when a 25 mm iliac total length is not feasible (due to its curtailment), progression of the graft to the external iliac artery must be considered. Alternatively, aorto-monoiliac stent grafts with femoro-femoral bypass and common contralateral iliac plug can be performed [28].

Diameter: A common iliac artery above 20 mm is considered to be aneurysmatic [13, 28]. Diameters of 20–24 mm can be treated with bell-bottom grafts (upon which the bottom-line diameter is enlarged to ensure distal sealing). Bell bottoms must be placed at the nearest level of the hypogastric ostium [28]. The larger graft limbs are of 28 mm, accessible in Ovation iX (Endologix Inc., Irvine, CA) and Endurant II (Medtronic Vascular Inc., Santa Rosa, CA) [29, 30]. However, as in proximal necks that tend to evolve to the degenerative wall progression associated with graft migration risk, this process may also happen in the distal neck [31]. Yet in the presence of aneurysmatic iliacs above the 24 mm diameter, the graft can be anchored in the external iliac artery, along with hypogastric trunk coil embolization to halt aneurysm backflow (type 2 endoleak) [13, 32, 33]. Still, preservation of one of the internal iliacs is advocated when both common iliacs are dilated and it can be reached with the use of branched devices (iliac side-branch device) or parallel/sandwich techniques [14, 34]. Bilateral hypogastric coil embolization comes with the risk of buttock claudication, sexual dysfunction, and, in extreme cases, colonic and medullar ischemia [2]. Staged procedures are justified and considered safe with reasonable morbidity [35, 36].

Angulation to aortic axis: Iliac tortuosity can be rectified with extra support guide wire or through-and-through technique (femorobraquial), granting uphold for the delivery system progression [13, 37]. Angulations closer than 90 degrees may make device progression and aneurysm sealing difficult, with risks of stent-graft kinking and thrombosis. It can be avoided in a crossed-legs deployment design, which, in addition to contralateral cannulation assistance, permits a longer length fixation of the limb and extra-column longitudinal support [28, 38].

3. Recommendations for EVAR graft choice

There are no current studies that compare the effectiveness of aneurysm exclusion between different endograft companies; some were performed only in observational studies. Moreover, the available data are always relatively obsolete due to constant improvements in technology and design.

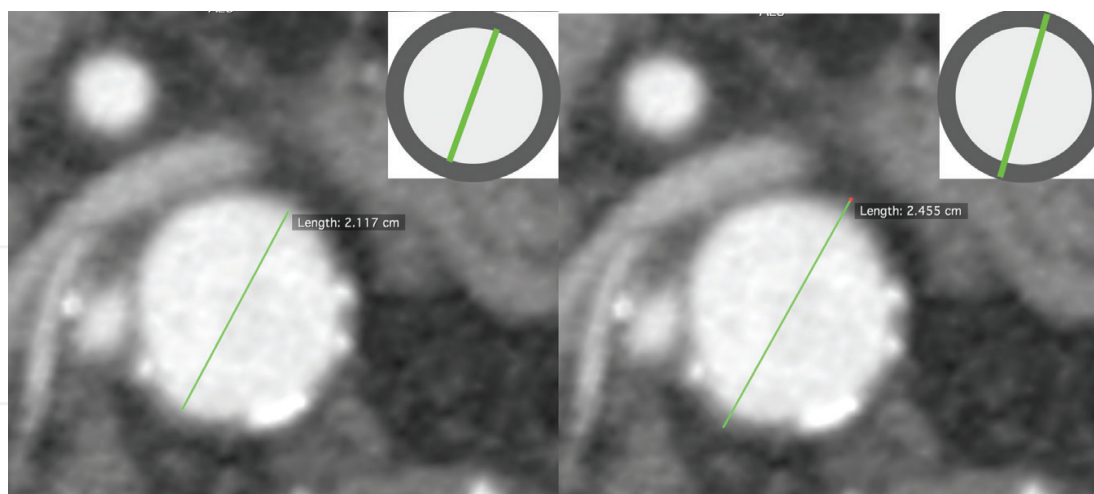


Figure 1. The inner-to-inner and outer-to-outer measurements.

Endograft	Material	Fixation	Barbs (Proximal Fixation)	# of pieces (not consider-ring iliac ex-tensions)	Available Main Body Sizes (Vessel Size Treated)	Available Iliac Limb Sizes (Vessel Size Treated)	Inner-to-inner/outer-to-outer wall diameter	Main Body Sheath Size (F)	IFU Advantages
Endurant II and IIs Medtronic	Polyester/Nitinol	Suprarenal	Yes	II. Main body CL limb IIs. Main body IpsiL limb CL limb	23-36mm (19-32mm)	10-28mm (8-24mm)	inner-to-inner	18-20	Necks \geq 10mm Angulated necks up to 75o
AFX Endologix	multilayer ePTFE/cobalt chromium	Suprarenal	No	Main bifurcated body Proximal extension	22-34mm (18-32mm)	16-25mm (10-23mm)	inner-to-inner	17	Anatomic fixation at iliac bifurcation Suits narrow distal aorta Access sheath
Excluder Gore	PTFE/Nitinol	Infrarenal	Yes	Main body CL limb	23-31mm (19-29mm) 32mm cuff available	10-27mm (8-25mm)	inner-to-inner	20	Repositionable main body (C3) Sheath w/ hemostatic valve
Zenith Flex Cook	Polyester/stainless steel	Suprarenal	Yes	Main body IpsiL limb CL limb	22-36mm (18-32mm)	8-24mm (8-20mm)	outer-to-outer	18-22	Stability Good radial force Detachable sheath
Ovation iX Endologix	PTFE/Nitinol	Suprarenal	Yes	Main body IpsiL limb CL limb	20-34mm (16-30mm)	10-28mm (8-25mm)	inner-to-inner	14-15	Proximal sealing rings Low profile
Aorfix Lombard	Polyester/Nitinol	Infrarenal	Yes	Main body CL limb	24-31mm (19-29mm)	10-20mm (8-19mm)	inner-to-inner	22	Angulated necks \leq 90
Incraft Cordis	Polyester/Nitinol	Suprarenal	No	Main body IpsiL limb CL limb	22-34mm (17-31mm)	10-24mm (7-22mm)	outer-to-outer	13-15	Ultra low profile
Treovance Bolton	Polyester/Nitinol	Suprarenal	Yes	Main body IpsiL limb CL limb	20-36mm (17-32mm)	8-24mm (8-20mm)	inner-to-inner	18-19	Necks \geq 10mm Angulated Detachable sheath
Anaconda Vascutek Terumo	Polyester/Nitinol	Infrarenal	Yes	Main body IpsiL limb CL limb	21,5-34mm (17,5-31mm)	10-23mm (8-20mm)	inner-to-inner	20-23	Repositionable main body Angulated necks \leq 90
E-Vita Abdominal XT Jotec	Polyester/Nitinol	Suprarenal	No	Main body CL limb	24-34mm (19-29mm)	12-22mm (11-23mm)	inner-to-inner	20	"Squeeze-to-release" controlled delivery

Table 1. Main Endografts available in the market and features descriptions based on IFU and orientations.

For the augment of EVAR graft-related durability, companies specify normatives presented in instructions for use (IFUs) with precise information regarding device sizing and deployment. They are based under the aneurysm’s morphologic parameters and rigorous bench

testing [39]. Patients with challenging anatomic presentations may benefit from a specific graft's design, delivery, and deployment attributes. Consequently, this requires a surgeon's better knowledge and experience for device selection [40]. In some cases although if in an attempt to embrace EVAR for patients not eligible for OSR the IFU are neglected it will result in significantly device failure in a mean 2 years of follow-up [39]. The most common IFU non-adherence situation is hostile neck anatomies: proximal and distal necks below 10 mm, angles over 60 degrees, diameters higher than 28 mm, thrombus or calcifications over 50% of the diameter, and conical presentations. These are said to have high aneurysmatic sac growth, early endoleak formation, and greater reintervention needs [41, 42].

An IFU compliance for each company guidance is imperative with regard to graft choice based on diameter measurements. Diameter dimensions can be calculated from intima to intima (inner wall) or adventitia to adventitia (outer wall) (**Figure 1**). When these details are not observed, the impacts on oversizing can be clinically expressive. Stent grafts with inner-wall measurement recommendations can be over-dimensioned if a 20% oversizing estimated from adventitia is considered. Inversely, devices with outer-wall assessment can be under-sized if estimated from intima. Because measurements are based on a static image of CTA (at any point of the cardiac course), these differences can be more problematic if diameter variations caused by aortic pulsatility seen on ECG-gated CT are considered [43].

Table 1 sums characteristics of endovascular devices according to their IFU, including diameter measurements recommendations.

4. The path to EVAR access sheaths: iliacs

Traditionally, the vascular access for EVAR performance is warranted by the direct puncture of the femoral artery under open surgery dissection [44]. Alternatively, the access can be obtained by an ultra-sound guided puncture of the common femoral artery in a non-diseased arterial segment (percutaneous technique) [45].

However, the pathway to EVAR cannot always present the favorable properties for sheath progression. Unfavorable sizes of the device diameters, marked tortuosity, or calcifications can prevent sheath progression augmenting the procedure's complexity. These alterations, when not identified in the pre-operative period, can lead to a significant rise in morbidity and mortality [46]. Iliac rupture is directly related to lethality and the necessity of immediate correction, which can jeopardize the intervention's final results. In the EUROSTAR registry, the most common cause of primary conversion is access failure, the main body graft sheath progression being the most responsible (the main body graft) [47].

Thus, the EVAR graft choice shall take into count the delivery component size, especially the main body graft, compared to the size of the vessel access (iliacs) that should be compatible. Considering that infrarenal grafts available in the market have delivery sheaths up to 24 F (while thoracic grafts are up to 28 F) [48], the lesser iliac diameters acceptable are between 7 mm and 8 mm. In addition not to display pronounced tortuosity (over 90 degrees), iliacs and femorals should not have calcifications that may lead to plaque dislodgement, vessel-wall lacerations, or arterial embolizations.

Although less frequent in daily practice, strategic alternatives are proposed for these morphologic adverse presentations.

Conduits are designated for small or calcified arteries (femorals/external iliacs) and the necessity of larger delivery sheaths (from 22F). Through an extraperitoneal exposure a 10 mm dacron graft is sewed terminal laterally to the common iliac (or bottom of the aorta, in cases of extreme iliac calcification) and externalized by counter opening in the groin, serving as a conduit for the device progression [49].

External iliac artery straightening: In very tortuous arteries, extraperitoneal dissection and manual rectification by traction of the iliac artery can favor sheath introduction and progression. By the end of the procedure, the redundant segment can be resected and the artery reconstructed [50].

Brachial artery catheterization: It consists of percutaneous access of the left brachial artery and a 035" wire passage (extra stiff of 300 cm or a 450 cm of a hydrophilic) with exteriorization through femoral access. The wire is then caudally pulled at the femoral site rectifying the tortuosity [51].

Endoconduits: The use of an diameter oversized covered stent, followed by vessel angioplasty, promoting an iliac "controlled rupture," in a way to allow passage of the delivery system [50, 52].

Hydrophilic dilators (Coons, Cook Medical) are available up to 22F. They can be introduced by femoral access and gently progressed over a stiff guide wire under radioscapy. One can estimate the delivery sheath behavior in an adverse iliac anatomy without necessarily contaminating the endograft [53]. They also can, in exception, be used for careful and gradual dilation of limiting-size iliacs.

5. Essential tools for planning and sizing with OsiriX/Horos

Table 2 sums the most important Region of Interest (ROI) tools for EVAR measuring and image manipulation that are most commonly used in OsiriX/Horos.

Some particularities of aneurysm measurements must be noticed: it is known that when two-dimensional (2D) images are used to evaluate 3D structures, like necks, it induces observers' measurements' variations [15]. To diminish the divergence, authors recommend that diameters should be estimated under a 3D reconstruction of the centerline lumen (CLL) [15, 54]. Some software can perform the centerline reconstruction automatically (like the Aquarius iNtuition and OsiriX, when the specific *EVAR plug-in/sovamed.com* or unofficial plug-ins like *CMIV CTA Tools* are installed) but intrinsic errors of self-regulating algorithms may occur. Because an automatically constructed centerline always follows the middle of contrast line, it won't observe the aortic axis in a saccular aneurysm, for example, deviating its route. By doing so, the transversal images perpendicular to the CLL may sometimes not represent the actual size of the vessel.

This is why concepts of central lumen flow (CLF) are used: It tends to considerate the preliminary location of the wire paths and endografts, along with aortic migration (**Figure 2**). For this

ROI Tool	Keyboard shortcut	Description	Advantages	Disadvantages
Magnifier	Z	Zoom In Zoom Out	Precise assessment to alterations of the vessel wall. Use for high definition view of inner-to-inner/outer-to-outer measurements within multislice CTA.	Image definition depends of CTA slice thickness.
Window Level and Width	W	Brightness and Contrast adjustment: manipulates the Hounsfield tissue density scale.	Modifies attenuation values of a tomographic image.	Wrong manipulation can lead to overestimate/underestimate arterial lesions.
Length	L	Distance measurement	Precise assessment for diameters	Operator dependant
Angle	A	Angle measurement	Precise assessment for aortic neck migration	Operator dependant
3D Point	P	Permanently marks the voxel in a volumetric serie of image	It preserves properties of depth and spatial positioning of the marked voxel. It can embody any particular structure of interest during a CTA study: vessels, arterial lesions, paths, etc.	Each point comes with an information box that can overlay and polute the studied image on a planar view (single axial or MPR).
Curved Path Reformation (3D curved MPR)		"Virtual Catheter" with measurements Creation mode: deploys simplified and structural model that originate the path. Edition mode: fine tuning of the created path in the three incidences.	Permits the manual construction of the Central Lumen Line (CLL) and Central Lumen Flow (CLF) Allow length measurements by navigating the A/B/C rulers along the path. Can simulate path and behavior of intraluminal catheters	Hard-working path construction of CLL/CLF for not familiarized users. Cannot give precise lengths between diameters if referential spots aren't marked previously (probability of interobserver error of judgement) Demands practice.

Table 2. Main basic tools of image manipulation for EVAR planning in OsiriX/Horos.

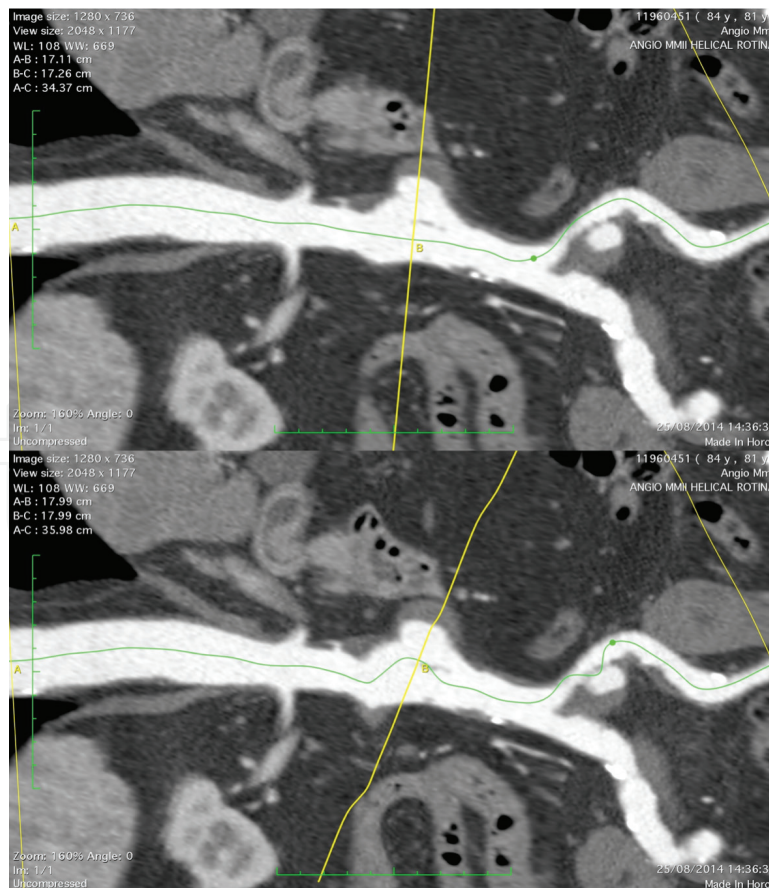


Figure 2. Central lumen line (CLL) construction (left) and Central lumen flow (CLF, right).

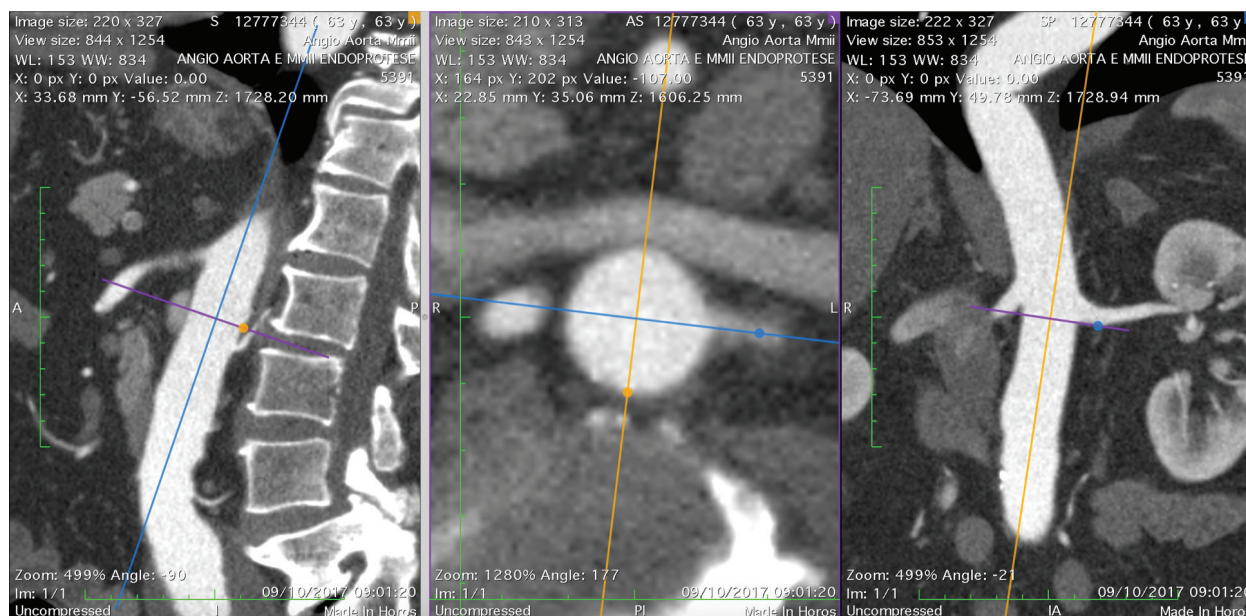


Figure 3. Orthogonal exposure of the aorta perpendicular to its axis, when sagittal and coronal planes are corrected.

reason, it seems justifiable that diameter measurements should instead be obtainable from orthogonal projections (CTA under 3D MPR reconstruction) (**Figure 3**) [6].

However, it is difficult to recognize the correspondent vessel segment assessed in MPR on a CLF-reconstructed image. This causes the length measurements not so precise if related directly to the different levels of aortic dimensions in an orthogonal view. For that reason, it is proposed that the orthogonal projections on MPR should be marked with the *3D Point* while determining aortic's widths. By doing so, the exact corresponding aortic segment is mark represented posteriorly in a curved-MPR centerline reformatting, promoting precise longitudinal dimensions (achievable by moving the rulers between two previously marked 3D points).

6. Planning EVAR: Neck total length exposure—The renal artery ostial projection technique

The intraoperative assessment for the stent-graft deployment is usually guided by aortic neck's angiography, which provides a 2D view prone to the parallax effect (an artifact caused by overlaying structures of different levels in a single image). Therefore, the proximal neck of AAA and/or too angulated iliac arteries may hinder accurate visualization of the ostium of the renal artery. A suboptimal positioning of the X-ray equipment for image capture can cause an overlapping of branches along with neck tortuosity, restraining the correct judgment and use of the entire neck's length for graft fixation and proximal sealing.

Thus, the finest way to prevent this artifact is by determining preoperatively the optimal intraoperative disposition of the fluoroscopy unit, with a perfectly perpendicular view to the origin of the LRA [22]. The technique described here is intended to promote the LRA visualization, exposed orthogonally to its emergence and perpendicularly to the aortic axis of

aneurysm's neck [55]. It offers an alternative to the Broeders and Blankensteijn technique [56], to the foreknowledge of the C-arm optimal positioning.

Using concepts of geometric correction and through the manipulation of DICOM images in OsiriX/Horos software, it is possible to trace the same angle of renal artery's ostial exposure in intraoperative 2D imaging (contrast angiography). The LRA ostial perpendicular view is obtained by 3D-MPR CTA reconstruction and the manipulation of sagittal and coronal layers in order to obtain the true axial image of the aorta. This exposure practically corrects any rotational effects of the aortic neck caused by tortuosity of AAA, with a near-perfect circumferential slice of the aorta.

The frame, that displays a slice 90 degree to the aortic axis, is then marked with the 3D *point* tool that allows a permanent voxel signal to the CTA volume. Three *points* are settled in an equilateral circumscribed triangle shape array [57] (one point in the anterior wall and two in the posterior), of which the anterior point is oriented by the tangent line of the LRA ostium. The *points*-marked voxels are then reproduced under a 3D-by-volume rendering, preserving their spatial properties [58]. As in spatial geometry, three points are always coplanar; and if a rotation of the 3D by volume promotes the *points* alignment along a single axis (and equidistant), an orthogonal exposure of aneurysm's neck related to the LRA is achieved (**Figure 4**) [55]. The angles that are necessary to reproduce the same ostial LRA exposure intraoperatively are automatically provided by the software (right corner of the 3D-by-volume rendering image). When these angles are recreated during radiosopic contrast angiography the images are alike (**Figure 5**). The deployment of endografts that has proximal markers (at least three) under this optimal angulation demonstrates them visible in a straight-line formation, just as when these markers are used to the C-arm gantry-angle fine-tuning [15]. Therefore, this technique allows the software to simulate these proximal marks (with the advantage of also exposing the renal artery ostia free of parallax).

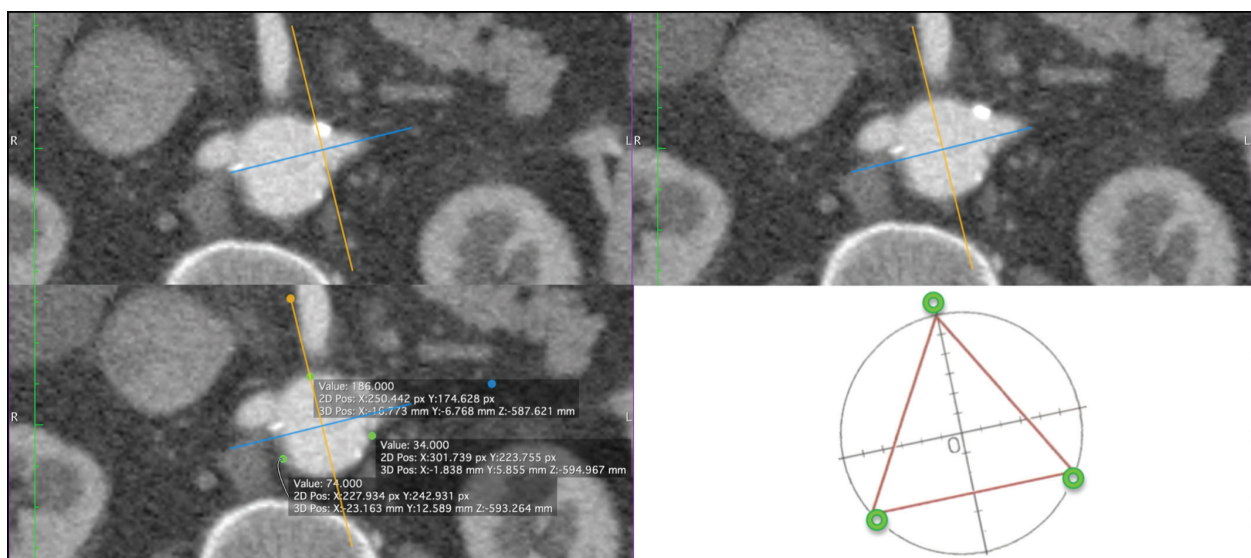


Figure 4. Above: tangent targeted from the projection of the LRA and intraluminal positioning for beginning 3D *point* marking. Below: construction of the equilateral circumscribed triangle and geometric representation of the points triangular array (for the exemplified case).

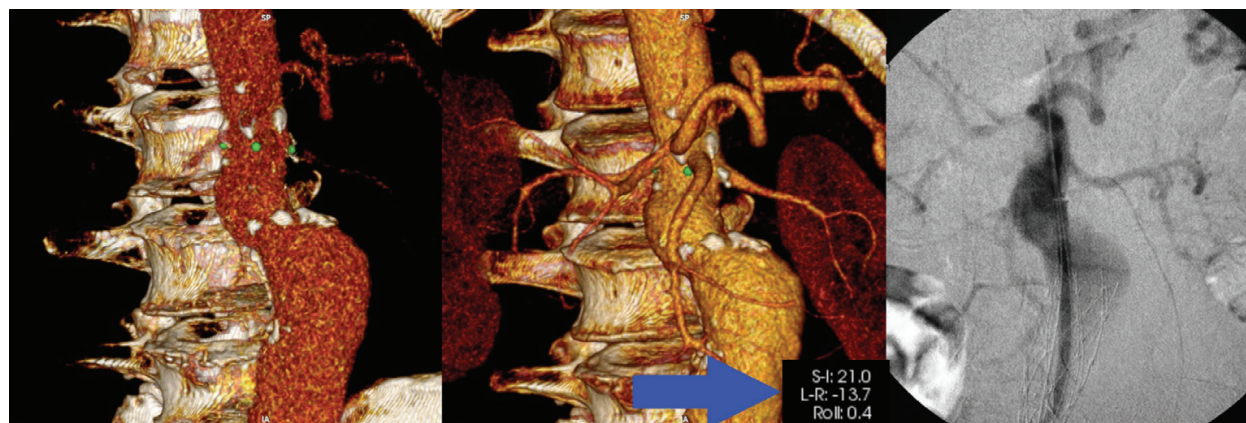


Figure 5. Alignment of the 3D *points* in 3D-by-volume rendering. The automatic angulation is provided automatically by the software (green arrow, right corner). When reproduced in the radioscopic device, the foreseen image and the intraoperative angiography are the same.

The closer is this fluoroscopic incidence correction to the software's tomographic reproduction, the more careful is the LRA visualization and the better the exploitation of aortic's neck for anchorage and sealing—and the more accurate is the endograft deployment. By applying these concepts of spatial geometry in order to systematically achieve the best angle for LRA ostial exposure, it is possible to reduce variations between different CTA examiners during EVAR planning. When ensuring the reproducibility of the technique, errors of personal interpretation are reduced.

7. Planning EVAR: The virtual fluoroscopy preset

In addition to precise measurement—such as diameters, lengths, and angles [7]—and the analysis of the characteristics of the aneurysm, it is possible to get a better use of information such as topographic positioning of visceral arteries and their respective references under a radioscopic view.

This technique grants the intraluminal placement prediction of angiographic catheters and radioscopic analysis during EVAR [58]. In a 3D-by-volume rendering, using the pre-defined bone CT reconstruction and the pencil preset, one can adapt and modify the tomographic values of windowing, color lookup table (CLUT), and shading which in turn define brightness, contrast, and color range of the image. At this new setting, the name of virtual fluoroscopy (VRF) can be assigned and recreated in other OsiriX/Horos platforms, becoming a replicable format (**Figure 6**).

Then, markings of the renal arteries on axial projections are performed (with the 3D *point* command). Again, the *points*-marked voxels (now embodied as renal vessels) are reproduced when submitted under any CTA reconstruction, preserving their volumetric properties. Once the exam is subjected to a 3D-by-volume rendering using this VRF preset, the renal arteries (and other visceral branches of interest that could be previously *pointed*) may be assessed in relation to a simulated fluoroscopy image (**Figure 7**).

Then, additional annotations can be made regarding the renal arteries' position referring to the vertebral axis. Also, guided by these images, it is possible to minutely predict aneurysm

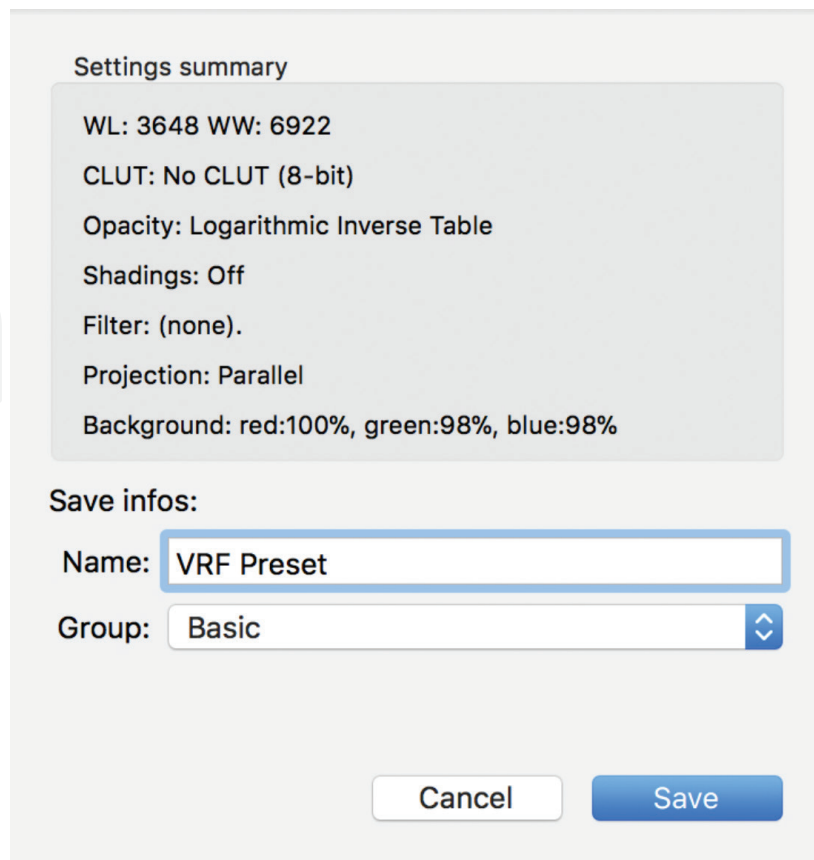


Figure 6. The Virtual Fluoroscopy Preset.

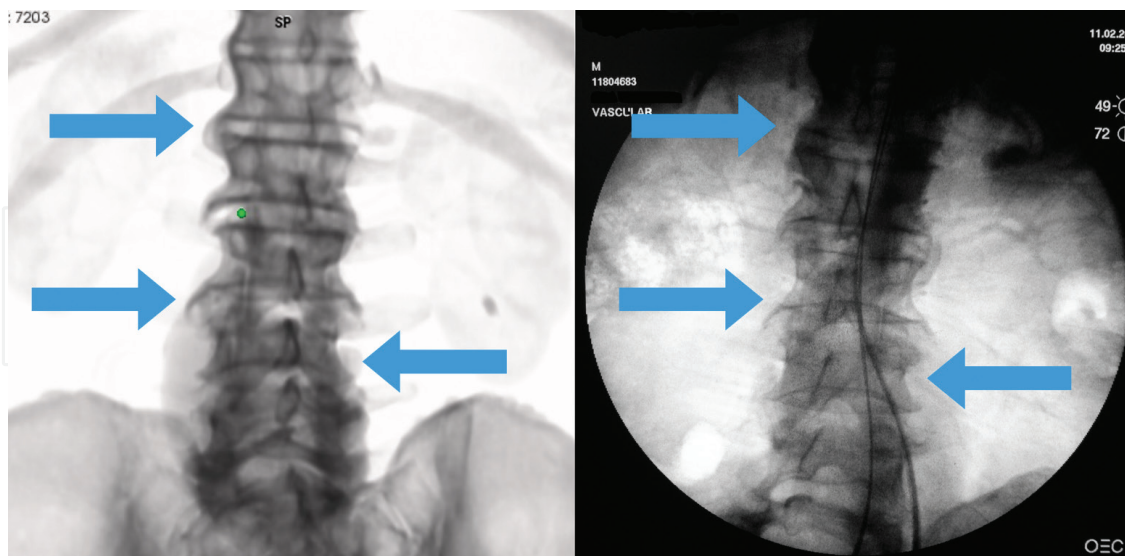


Figure 7. The Virtual Fluoroscopy and its correlation to the intraoperative fluoroscopy.

neck location (when under intraoperative fluoroscopy acquisition), as well as estimate the ideal positioning of the diagnostic catheters for digital subtraction angiography (DSA) at the moment of stent-graft deployment. Vertebral osteo-degenerative alterations identified in VRF can easily be recognized intraoperatively, enhancing vessel navigation without the necessity

of consecutive angiographies so as to identify visceral branches' position. In addition, an improved position of the C-arm unit so as to reduce the interference from the parallax effect is foreseen (**Figure 8**).

However, the ideal positioning of the X-ray equipment during the surgical procedure may be different than expected during the preoperative study. It is considered that the aneurysm neck can possibly shorten or lengthen higher than expected in the intraoperative, because of the influence of inserted extra-support guide wires or the endograft itself [59]. Even so, although aneurysm's neck angulation, can change the ostial position of renal arteries/visceral branches does not expressively shift [22, 60]. This does not compromise comparisons between images formed by the VRF preset from those radioscopically composed, but this difference can be significant if fusion of pre procedural images are overlaid to real time fluoroscopy (VRF vs. fluoro) [60].

The 3D-by-volume rendering adjusts the voxel's attenuation coefficient at a scale of color and degree of opacity (transparency) along the axes. Thus, it preserves information of depth and shows better spatial distribution of structures along with an enhanced-by-light (shading) 3D effect [7]. The manipulation of these data (the dose distribution radiated to a surface) allows the visualization of the maximum intensity projection (MIP), which demonstrates the densest voxel (higher attenuation coefficient). They are displayed as opaque areas of high contrast (as bone surfaces) and as transparent values of low attenuation (soft tissues). Even if there are overlaid images of different depths in the same drawing (i.e., structures that when superimposed compete with the density of others of interest, like the aorta), this is a "desirable" effect when the aim is to simulate a gray-scale CTA image of a single bi-planar fluoroscopy.

Carefully, by studying the CTA under VRF, one can reduce the number of intraoperative angiographies in an attempt to obtain the best angiographic capture that provides the location of renal arteries and aneurysm neck for graft deployment. The closer is this angiographic reproduction to virtual fluoroscopy, the more careful is the surgeon's inspection of the renal arteries' location and the better will be the use of aneurysm neck for fastening and sealing

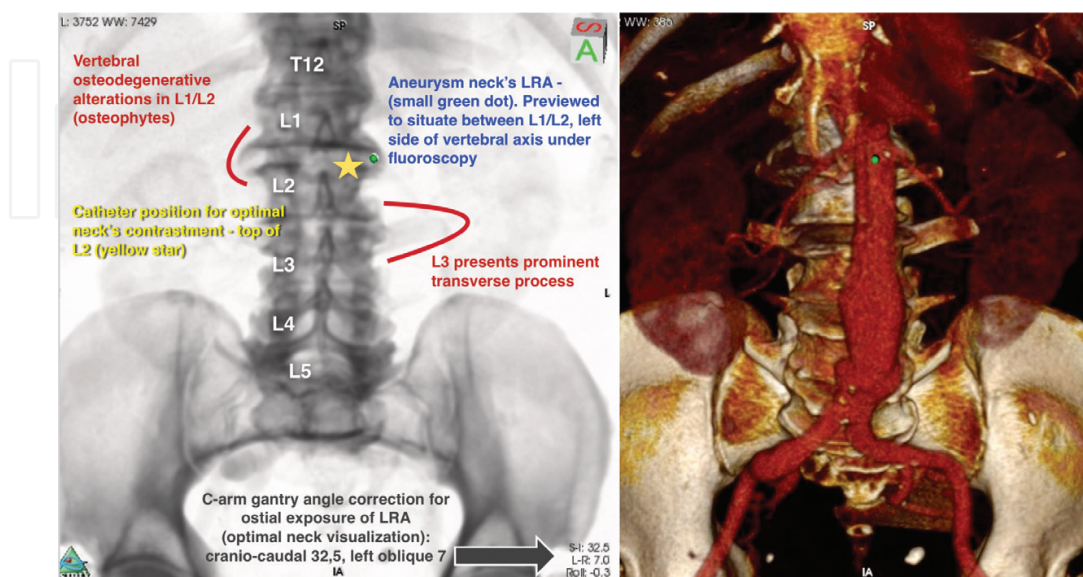


Figure 8. The complete “beyond basics” study of CTA.

endoprosthesis; being more accurate EVAR execution while the total volume of contrast used is smaller and reducing renal overload in vulnerable patients. Consequently, optimizing these surgical steps comes also with lesser radiation dose exposure.

8. Routine for EVAR planning and sizing

These steps are the same used at the Vascular Surgery Department (the University of Campinas, Brazil) and validated prospectively in 2015 [61].

- a 3D-MPR view of thick coronal slice with renal artery exhibition and aortic iliac axis;
- a sketch of the obtained figure in an individualized sheet, with the patient's personal data and surgical details (date, performing physician, surgical team, etc.);
- recognition of the LRA (which is posteriorly confirmed after centerline construction);
- angle definition of the aortic neck to the suprarenal axis, aortic aneurysm, and iliac axis in 3D MPR;
- diameter measurements in orthogonal 3D-MPR exposure, perpendicular to aortic axis and oriented to the inner curve of the artery;
 - the aortic width above the uppermost renal artery;
 - diameters along aneurysm's neck, starting immediately after the LRA—from 3 to 5 measurements (for non-cylindrical necks). Segments where the difference between proximal and distal widths are above 15% for cylindrical and 20% for reverse-tapered shapes should not be considered as part of the necks;
 - the largest AAA diameter;
 - the distal aortic diameter (pre-bifurcation) and distal lumen aortic width;
 - diameters along the right-common iliac artery, from 3 to 5 measurements (for non-cylindrical iliacs);
 - diameters along the left-common iliac artery, from 3 to 5 measurements (for non-cylindrical iliacs);
 - diameters of external iliacs and common femorals (access vessels study);
- Voxel signaling with the 3D *Point* tool of the aortic lumen, at the center, in an orthogonal perpendicular view:
 - immediately after the LRA (aortic neck's first measurement);
 - the lowest aortic neck's diameter;
 - at the aortic bifurcation;
 - at the emergence of hypogastric ostium bilaterally;

- the CLF construction in curved 3D-MPR with the curved path reformation (CPR) tool.
 - Creation Mode: It is an outline draft disposure of aortic flow essential to the path oriented by the slightly inner curve in angulated aneurysms.
 - Editing Mode: It is the fine tuning of the centerline, between two previously constructed orientation marks.
 - Length measurements are obtained by positioning the vertical rulers along the centerline (from A to B, from B to C, or from A to C). When the mouse cursor moves along the reformed centerline image a highlighted correspondent dot moves along the CPR path in the three planes (axial, sagittal, and coronal). The measuring bars A/B/C are positioned over the previously 3D *pointed* (marked) references (previous step): *points* after the LRA and the lowest aortic neck measurement/the aneurysm extension/the common iliac segments/the infrarenal distance to aortic bifurcation and to hypogastric ostium, bilaterally (**Figure 9**).
- C-arm gantry angle obtainment for neck visualization with LRA ostium exposure by the triangulation technique.

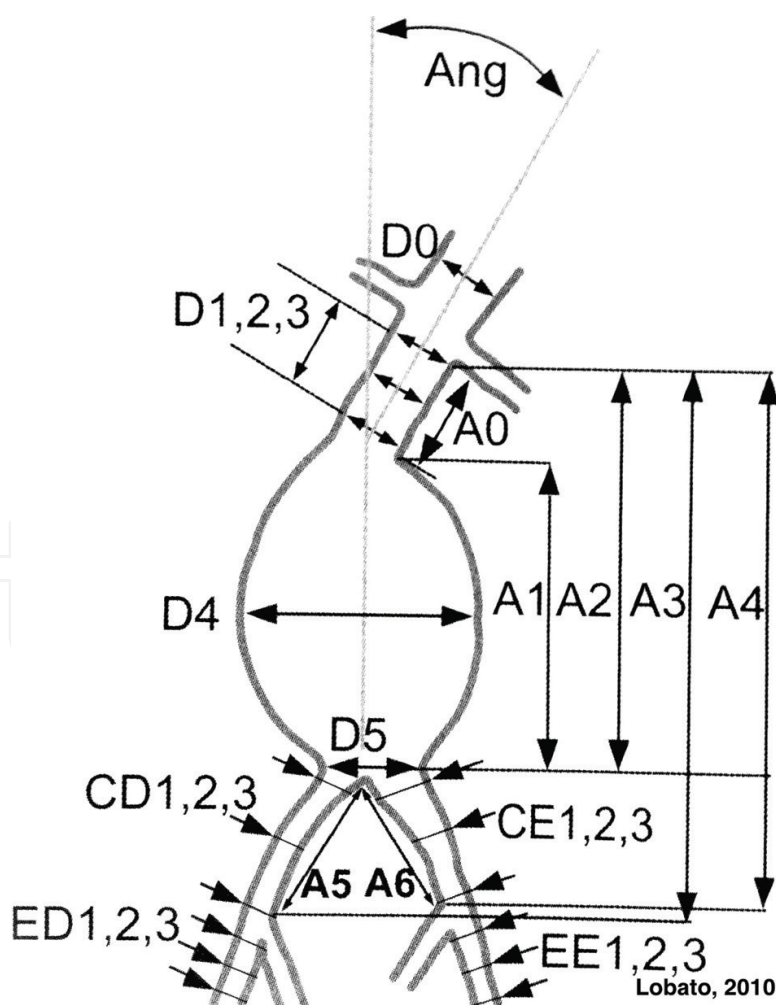


Figure 9. Summary of EVAR sizing.

- The positioning of renal arteries and aneurysm's neck itself is related to the vertebral axis, as long as one can anticipate the optimal positioning of angiographic catheters for image acquisition, by the VRF preset.

9. Conclusions

The use of OsiriX/Horos as a complementary tool allows doctors to assist in the preparation of surgeries (as endovascular) extending it beyond the field of diagnostic radiology. These tasks can be easily incorporated into the armamentarium of the surgeon to avoid pitfalls and unforeseen situations that are identified intraoperatively, increasing the operatory risk and often times leading to intervention failure.

This chapter presents simple techniques which are of great practical importance in planning interventional treatments. The ability to manipulate digital formats of medical images allows the recovery of a larger volume of data and grants that interventional procedures can be performed more efficiently, with less time for image projection adjustment, contrast injections, and exposure to ionizing radiation. As a result, one can obtain the impact in relation to the improvement of the surgical technique, translated into the less use of contrast, reduced surgical time, and intraoperative bleeding.

New ways to adapt this software have increased by expanding its use to new tasks. Our proposal is to create the familiarity of professionals and encourage demystified practice of this computer program, an essential tool in surgical planning, where more and more procedures are guided by images.

Acknowledgements

We thank Dr Ana Terezinha Guillaumon, M.D., Ph.D., Chief of the Division of Vascular Surgery of the University of Campinas Surgery Department, because of whom the implantation of these protocols was possible and we had full unrestricted support.

Conflict of interest

None.

Author details

Giovani José Dal Poggetto Molinari

Address all correspondence to: drgiovani.molinari@uol.com.br

University of Campinas, Campinas, Brazil

References

- [1] Parodi JC, Ferreira LM. Ten-year experience with endovascular therapy in aortic aneurysms. *Journal of the American College of Surgeons*. 2002;**194**(1 Suppl):S58-S66
- [2] Chaikof EL, Brewster DC, Dalman RL, Makaroun MS, Illig KA, Sicard GA, et al. SVS practice guidelines for the care of patients with an abdominal aortic aneurysm: Executive summary. *Journal of Vascular Surgery*. 2009;**50**(4):880-896
- [3] Arhuidese IJ, Salami A, Obeid T, Qazi U, Abularrage CJ, Black JH, et al. The age effect in increasing operative mortality following delay in elective abdominal aortic aneurysm repair. *Annals of Vascular Surgery*. 2015;**29**(6):1181-1187
- [4] Wyers MC, Fillinger MF, Schermerhorn ML, Powell RJ, Rzucidlo EM, Walsh DB, et al. Endovascular repair of abdominal aortic aneurysm without preoperative arteriography. *Journal of Vascular Surgery*. 2003;**38**(4):730-738
- [5] Espinosa G, Marchiori E, Araújo AP, Caramalho MF, Barzola P. Abdominal aorta morphometric study for endovascular treatment of aortic aneurysms: Comparison between spiral CT and angiography. *Revista brasileira de cirurgia cardiovascular: orgao oficial da Sociedade Brasileira de Cirurgia Cardiovascular*. 2002;**17**(4):323-330
- [6] de Almeida Sandri G, Ribeiro MS, Macedo TA, Vrtiska T, Oderich GS. Planning endovascular aortic repair with standard and fenestrated-branched endografts. *The Journal of Cardiovascular Surgery*. 2017;**58**(2):204-217
- [7] Kuroki IR, Magalhães FV, Rizzi P, Coreixas IMH. Angiotomografia. In: Brito CJ, editor. *Cirurgia Vascular: cirurgia endovascular, angiologia*. 3a ed. Rio de Janeiro: Revinter; 2013. pp. 438-496
- [8] Ferreira MMDV, Azevedo LL, d'Utra GN, Cunha RS. Aneurismas da Aorta Torácica e Toracoabdominal - Tratamento Endovascular. In: Brito CJ, editor. *Cirurgia Vascular: cirurgia endovascular, angiologia*. 3a ed. Rio de Janeiro: Revinter; 2013. pp. 689-736
- [9] Walls MC, Thavendiranathan P, Rajagopalan S. Advances in CT angiography for peripheral arterial disease. *Cardiology Clinics*. 2011;**29**(3):331-340
- [10] Pitoulias GA, Donas KP, Schulte S, Aslanidou EA, Papadimitriou DK. Two-dimensional versus three-dimensional CT angiography in analysis of anatomical suitability for stent graft repair of abdominal aortic aneurysms. *Acta Radiologica*. 2011;**52**(3):317-323
- [11] Walker TG, Kalva SP, Ganguli S, Oklu R, Salazar GM, Waltman AC, et al. Image optimization during endovascular aneurysm repair. *AJR American Journal of Roentgenology*. 2012;**198**(1):200-206
- [12] Rousseau H, Chabbert V, Maracher MA, El Aassar O, Auriol J, Massabuau P, et al. The importance of imaging assessment before endovascular repair of thoracic aorta. *European journal of vascular and endovascular surgery: the official journal of the European Society for Vascular Surgery*. 2009;**38**(4):408-421

- [13] Ristow A, Vescovi A, Massière BV, Correa MP, Paludetto G. Aneurisma da Aorta Abdominal - Tratamento pela Técnica Endovascular. In: Brito CJ, editor. *Cirurgia Vascular: cirurgia endovascular, angiologia*. 3a ed. Rio de Janeiro: Revinter; 2013. pp. 799-877
- [14] Lobato AC. Aneurisma de Aorta Infrarrenal. In: Lobato AC, editor. *Cirurgia Endovascular*. 2nd ed. São Paulo: Instituto de Cirurgia Vascular e Endovascular de São Paulo; 2010
- [15] de Vries JP. The proximal neck: The remaining barrier to a complete EVAR world. *Seminars in Vascular Surgery*. 2012;**25**(4):182-186
- [16] Wang S, Hicks CW, Malas MB. Neck diameter and inner curve seal zone predict endograft-related complications in highly angulated necks after endovascular aneurysm repair using the Aorfix endograft. *Journal of Vascular Surgery*. 2017
- [17] O'Neill S, Collins A, Harkin D. Limb occlusion after endovascular repair of an abdominal aortic aneurysm: Beware the narrow distal aorta. *Irish Journal of Medical Science*. 2012;**181**(3):373-376
- [18] Kalef-Ezra JA, Karavasilis S, Kouvelos G, Dristiliaris D, Michalis LK, Matsagkas M. Endovascular abdominal aortic aneurysm repair: Methods of radiological risk reduction. *The Journal of Cardiovascular Surgery*. 2011;**52**(6):769-778
- [19] van Keulen JW, Moll FL, Tolenaar JL, Verhagen HJ, van Herwaarden JA. Validation of a new standardized method to measure proximal aneurysm neck angulation. *Journal of Vascular Surgery*. 2010;**51**(4):821-828
- [20] Ltd. V. Anaconda ONE-LOK Stent Graft System. Anaconda Iliac Stent Graft System. Anaconda AAA Stent Graft System Aortic Cuff. Instructions for Use
- [21] Lombard I. Instructions for use. Aorfix AAA flexible stent graft system and Aorfix plus AAA flexible stent graft system. With Aorflex Delivery Device
- [22] van Keulen JW, Moll FL, van Herwaarden JA. Tips and techniques for optimal stent graft placement in angulated aneurysm necks. *Journal of Vascular Surgery*. 2010;**52**(4):1081-1086
- [23] van Prehn J, Schlosser FJ, Muhs BE, Verhagen HJ, Moll FL, van Herwaarden JA. Oversizing of aortic stent grafts for abdominal aneurysm repair: A systematic review of the benefits and risks. *European journal of vascular and endovascular surgery: the official journal of the European Society for Vascular Surgery*. 2009;**38**(1):42-53
- [24] Baumann F, Ganghi R, Pena C, Katzen B. Principia's Gerais do Tratamento dos Aneurismas de Aorta Torácica e Abdominal. In: Carnevale FC, editor. *Tratado de Radiologia Intervencionista e Cirurgia Endovascular*. 1a ed. Rio de Janeiro: Thieme Revinter Publicações; 2017
- [25] Ihara T, Komori K, Banno H, Kodama A, Yamamoto K, Sugimoto M. Relationship between the distal migration and length of the distal landing zone after endovascular aneurysm repair (EVAR). *Surgery Today*. 2016;**46**(1):56-61
- [26] Heikkinen MA, Alsac JM, Arko FR, Metsanoja R, Zvaigzne A, Zarins CK. The importance of iliac fixation in prevention of stent graft migration. *Journal of Vascular Surgery*. 2006;**43**(6):1130-1137. discussion 7

- [27] Waasdorp EJ, de Vries JP, Sterkenburg A, Vos JA, Kelder HJ, Moll FL, et al. The association between iliac fixation and proximal stent-graft migration during EVAR follow-up: Mid-term results of 154 Talent devices. *European journal of vascular and endovascular surgery: the official journal of the European Society for Vascular Surgery*. 2009;**37**(6): 681-687
- [28] Zarins CK, Waasdorp E. Opções Técnicas para Correção Endovascular do Aneurisma da Aorta Abdominal com Artéria Iílica Comum Ectásica, Aneurismática ou Curta. In: Lobato AC, editor. *Tratamento Endovascular das Complicações Aorto-Iílicas*. 1st ed. São Paulo: Instituto de Cirurgia Vascular e Endovascular de São Paulo; 2008
- [29] Inc. MV. Endurant II AAA Stent Graft System: Instructions for Use; 2015
- [30] Trivascular I. Ovation prime abdominal stent graft system with the ovation iX iliac stent graft. Instructions for Use. 2015
- [31] Kaladji A, Cardon A, Laviolle B, Heautot JF, Pinel G, Lucas A. Evolution of the upper and lower landing site after endovascular aortic aneurysm repair. *Journal of Vascular Surgery*. 2012;**55**(1):24-32
- [32] Mehta M, Veith FJ, Ohki T, Cynamon J, Goldstein K, Suggs WD, et al. Unilateral and bilateral hypogastric artery interruption during aortoiliac aneurysm repair in 154 patients: A relatively innocuous procedure. *Journal of Vascular Surgery*. 2001;**33**(2 Suppl):S27-S32
- [33] Parlani G, Zannetti S, Verzini F, De Rango P, Carlini G, Lenti M, et al. Does the presence of an iliac aneurysm affect outcome of endoluminal AAA repair? An analysis of 336 cases. *European journal of vascular and endovascular surgery: the official journal of the European Society for Vascular Surgery*. 2002;**24**(2):134-138
- [34] Saengprakai W, van Herwaarden JA, Georgiadis GS, Slisatkorn W, Moll FL. Clinical outcomes of hypogastric artery occlusion for endovascular aortic aneurysm repair. *Minimally Invasive Therapy & Allied Technologies*. 2017;**26**(6):362-371
- [35] Criado FJ, Wilson EP, Velazquez OC, Carpenter JP, Barker C, Wellons E, et al. Safety of coil embolization of the internal iliac artery in endovascular grafting of abdominal aortic aneurysms. *Journal of Vascular Surgery*. 2000;**32**(4):684-688
- [36] Wolpert LM, Dittrich KP, Hallisey MJ, Allmendinger PP, Gallagher JJ, Heydt K, et al. Hypogastric artery embolization in endovascular abdominal aortic aneurysm repair. *Journal of Vascular Surgery*. 2001;**33**(6):1193-1198
- [37] Al Shammari M, Taylor P, Reidy JF. Use of through-and-through guidewire for delivering large stent-grafts into the distal aortic arch. *Cardiovascular and Interventional Radiology*. 2000;**23**(3):237-238
- [38] Ramaiah VG, Thompson CS, Shafique S, Rodriguez JA, Ravi R, DiMugno L, et al. Crossing the limbs: A useful adjunct for successful deployment of the AneuRx stent-graft. *Journal of endovascular therapy: an official journal of the International Society of Endovascular Specialists*. 2002;**9**(5):583-586

- [39] Herman CR, Charbonneau P, Hongku K, Dubois L, Hossain S, Lee K, et al. Any nonadherence to instructions for use predicts graft-related adverse events in patients undergoing elective endovascular aneurysm repair. *Journal of Vascular Surgery*. 2018;**67**(1):126-133
- [40] Bastos Goncalves F, Rouwet Ellen V, Metz R, Hendriks JM, Vrancken Peeters M, Muhs BE, et al. Device-specific outcomes after endovascular abdominal aortic aneurysm repair. *The Journal of Cardiovascular Surgery*. 2010;**51**(4):515-531
- [41] Aburahma AF, Campbell JE, Mousa AY, Hass SM, Stone PA, Jain A, et al. Clinical outcomes for hostile versus favorable aortic neck anatomy in endovascular aortic aneurysm repair using modular devices. *Journal of Vascular Surgery*. 2011;**54**(1):13-21
- [42] Schanzer A, Greenberg RK, Hevelone N, Robinson WP, Eslami MH, Goldberg RJ, et al. Predictors of abdominal aortic aneurysm sac enlargement after endovascular repair. *Circulation*. 2011;**123**(24):2848-2855
- [43] Iezzi R, Dattesi R, Pirro F, Nestola M, Santoro M, Snider F, et al. CT angiography in stent-graft sizing: Impact of using inner vs. outer wall measurements of aortic neck diameters. *Journal of endovascular therapy: an official journal of the International Society of Endovascular Specialists*. 2011;**18**(3):280-288
- [44] Phade SV, Garcia-Toca M, Kibbe MR. Techniques in endovascular aneurysm repair. *International Journal of Vascular Medicine*. 2011;**2011**:964250
- [45] Lee WA, Brown MP, Nelson PR, Huber TS. Total percutaneous access for endovascular aortic aneurysm repair ("Preclose" technique). *Journal of Vascular Surgery*. 2007;**45**(6):1095-1101
- [46] Peterson BG, Matsumura JS. Creative options for large sheath access during aortic endografting. *Journal of Vascular and Interventional Radiology: JVIR*. 2008;**19**(6 Suppl):S22-S26
- [47] Cuypers PW, Laheij RJ, Buth J. Which factors increase the risk of conversion to open surgery following endovascular abdominal aortic aneurysm repair? The EUROSTAR collaborators. *European journal of vascular and endovascular surgery: the official journal of the European Society for Vascular Surgery*. 2000;**20**(2):183-189
- [48] Murray D, Ghosh J, Khwaja N, Murphy MO, Baguneid MS, Walker MG. Access for endovascular aneurysm repair. *Journal of endovascular therapy: an official journal of the International Society of Endovascular Specialists*. 2006;**13**(6):754-761
- [49] Criado FJ. Iliac arterial conduits for endovascular access: Technical considerations. *Journal of endovascular therapy: an official journal of the International Society of Endovascular Specialists*. 2007;**14**(3):347-351
- [50] Yano OJ, Faries PL, Morrissey N, Teodorescu V, Hollier LH, Marin ML. Ancillary techniques to facilitate endovascular repair of aortic aneurysms. *Journal of vascular surgery*. 2001;**34**(1):69-75
- [51] Criado FJ, Wilson EP, Abul-Khoudoud O, Barker C, Carpenter J, Fairman R. Brachial artery catheterization to facilitate endovascular grafting of abdominal aortic aneurysm: Safety and rationale. *Journal of Vascular Surgery*. 2000;**32**(6):1137-1141

- [52] Wu T, Carson JG, Skelly CL. Use of internal endoconduits as an adjunct to endovascular aneurysm repair in the setting of challenging aortoiliac anatomy. *Annals of Vascular Surgery*. 2010;**24**(1):114 e7-114e11
- [53] Criado FJ, Gashti M. Técnicas de Acesso Vascular no Implante de Endoprótese Aórtica: como evitar problemas e prevenir complicações. In: Lobato AC, editor. *Tratamento Endovascular das Complicações Aorto-Iliacas*. 1st ed. São Paulo: Instituto de Cirurgia Vascular e Endovascular de São Paulo; 2008
- [54] Gisbert SMM, Garcia JMZ, Palonés FJG, Juan PB, Montoya MR, Monzón EO. Diferencias entre la planificación del tratamiento endovascular de aneurismas de aorta abdominal con reconstrucción tridimensional vs tomografía computarizada y angiografía, y su impacto clínico. *Angiología*. 2014;**66**(4):183-189
- [55] Molinari GJ, Dalbem AM, Menezes FH, Guillaumon AT. Proposal of renal artery's ostial projection under virtual geometric correction in infrarenal aneurysms: Initial results of a pilot study. *Revista brasileira de cirurgia cardiovascular: orgao oficial da Sociedade Brasileira de Cirurgia Cardiovascular*. 2014;**29**(1):78-82
- [56] Broeders IA, Blankensteijn JD. A simple technique to improve the accuracy of proximal AAA endograft deployment. *Journal of endovascular therapy: an official journal of the International Society of Endovascular Specialists*. 2000;**7**(5):389-393
- [57] Rigonatto M. Triângulo equilátero inscrito numa circunferência. [cited 2013 May 22]. Available from: <http://www.mundoeducacao.com/matematica/triangulo-equilatero-inscrito-numa-circunferencia.htm>
- [58] Molinari GJ, Dalbem AM, Guillaumon AT. The use of virtual resources in preoperative preparation of infrarenal aneurysms: Exploring the OsiriX's potential. *Revista brasileira de cirurgia cardiovascular: orgao oficial da Sociedade Brasileira de Cirurgia Cardiovascular*. 2014;**29**(2):279-284
- [59] Oderich GS, Malgor RD. Aneurisma da Aorta toracoabdominal. In: Lobato AC, editor. *Cirurgia Endovascular*. 2nd ed. São Paulo: Instituto de Cirurgia Vascular e Endovascular de São Paulo; 2010. pp. 695-742
- [60] Maurel B, Hertault A, Gonzalez TM, Sobocinski J, Le Roux M, Delaplace J, et al. Evaluation of visceral artery displacement by endograft delivery system insertion. *Journal of endovascular therapy: an official journal of the International Society of Endovascular Specialists*. 2014;**21**(2):339-347
- [61] Molinari GJ, Guillaumon AT, Dalbem AM. Efficacy analysis of a script-based guide for EVAR execution: Is it possible to reduce patient exposure to contrast, operative time and blood loss even when advanced technologies are not available? *Brazilian Journal of Cardiovascular Surgery*. 2015;**30**(6):650-656